NOTES AND CORRESPONDENCE

Atmospheric Vacillations in a General Circulation Model. III: Analysis using Transformed Eulerian-Mean Diagnostics

DAVID J. KAROLY

Australian Numerical Meteorology Research Centre, Melbourne, 3001, Victoria, Australia

19 February 1982 and 2 July 1982

ABSTRACT

The vacillatory behavior of the general circulation model described by Hunt (1978a,b) is analyzed using transformed Eulerian-mean diagnostics. This model was shown by Hunt to have large time variations in the troposphere and stratosphere with a period of ~20 days. These diagnostics are used to show the coupling between the troposphere and the stratosphere and the forcing of mean state changes during the vacillation cycle.

The time variations of the wave-induced force on the mean flow and the Coriolis torque are in approximate balance throughout the vacillation cycle. Thus mean flow changes are small and the effect of the mean state on wave propagation is approximately constant. The vacillation cycle in the model is apparently due to variations in baroclinic wave activity in the troposphere and not to wave, mean flow interaction in the upper troposphere and stratosphere.

1. Introduction

In two earlier papers (Hunt 1978a,b; hereafter referred to as I and II), the vacillatory behavior of a general circulation model of the troposphere and stratosphere was analyzed. In I, the large-scale energy cycle of the model was shown to have large time variations with a period of ~20 days, particularly in the eddy kinetic and available potential energies. The transient behavior of the model stratosphere and its relationship to fluctuations in the coupling between the troposphere and stratosphere were investigated in II.

As an extension to I and II, the role of wave, mean flow interaction in the model vacillation cycle is studied here from the transformed Eulerian-mean viewpoint. This involves the description of the mean flow and temperature evolution using the transformed Eulerian-mean equations presented by Andrews and McIntyre (1976), and the use of the Eliassen–Palm (EP) cross section, presented by Edmon *et al.* (1980), as a diagnostic of waves on the mean flow. These diagnostics are able to show the effect of waves on the mean flow evolution and the effect of the mean flow on the pattern of wave propagation. The theory and use of these diagnostics has been reviewed by Edmon *et al.* (1980) and readers are referred to that paper for background, further details and earlier references.

The formulation of the diagnostics used here follows that of Dunkerton *et al.* (1981), where they were used to study the evolution of a stratospheric warming in a numerical model simulation. The quasi-geostrophic approximation to the transformed Eulerian-mean equations on the sphere for the zonal-mean zonal flow and temperature can be written, using standard notation, as

$$\bar{u}_t - f\bar{v}^* = \bar{X} + \nabla \cdot \mathbf{F}/(\rho_0 a \cos\phi) \tag{1}$$

and

$$\bar{\theta}_t + \bar{\theta}_z \bar{w}^* = \bar{Q}, \tag{2}$$

with $\rho_0 = \rho_0(z) = \rho_s e^{-z/H}$. The vertical coordinate is log-pressure $z = H \ln(p_s/p)$, with $p_s = 1000$ mb a reference pressure, H a constant and ρ_s a reference density. Since the model atmosphere is not isothermal, the density scale height in the model is not constant and z is not equal to physical height. However, choosing a typical value for the scale height, $H = 7$ km, means that the pressure altitude z differs by only a small amount from the physical height. The residual meridional circulation $(\bar{v}^*, \bar{w}^*)$ is defined by

$$\left.\begin{aligned} \bar{v}^* &= \bar{v} - \frac{1}{\rho_0}\frac{\partial}{\partial z}(\rho_0 \overline{v'\theta'}/\bar{\theta}_z) \\ \bar{w}^* &= \bar{w} + \frac{1}{a\cos\phi}\frac{\partial}{\partial \phi}(\cos\phi \overline{v'\theta'}/\bar{\theta}_z) \end{aligned}\right\}. \tag{3}$$

The EP flux divergence is

$$\nabla \cdot \mathbf{F} = \frac{1}{a\cos\phi}\frac{\partial}{\partial\phi}[F_{(\phi)}\cos\phi] + \frac{\partial}{\partial z}[F_{(z)}], \tag{4}$$

where the quasi-geostrophic approximation to the EP

0022-4928/82/122916-07$05.75

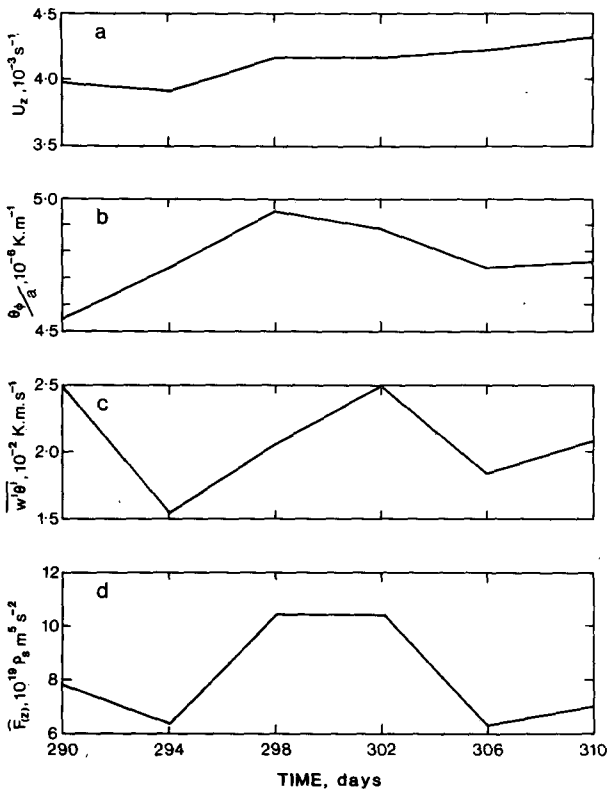

FIG. 1. Time variation of indicators of baroclinic wave activity in the troposphere. The data are averaged over nonoverlapping four-day periods centered at the values shown on the time axis. (a) Vertical shear of zonal wind $\bar{u}_z$ between 284 and 757 mb (z = 8.8 to 1.9) at 21° in units of 10^{-3} s^{-1}. (b) Meridional temperature gradient $\bar{\theta}_\phi/a$ between 63 and 15° at 757 mb (z = 1.9) in units of 10^{-6} K m^{-1}. (c) Vertical wave heat flux $\overline{v'\theta'}$ averaged over the zonal band from 51 to 39° and from 626 to 516 mb (z = 3.3 to 4.6) in units of 10^{-2} K m s^{-1}. (d) Vertical EP flux, $\hat{F}_{(z)}$, averaged over the zonal band from 51 to 39° and from 424 to 348 mb (z = 6.0 to 7.4) in units of 10^{19} ρ_sm^5 s^{-2}.

flux $\mathbf{F} = [F_{(\phi)}, F_{(z)}]$ is

$$\left.\begin{aligned} F_{(\phi)} &= -\rho_0 a \cos\phi \overline{u'v'} \\ F_{(z)} &= \rho_0 f a \cos\phi \overline{v'\theta'}/\bar{\theta}_z \end{aligned}\right\}. \tag{5}$$

The overbar indicates a zonal mean, primed variables are deviations from the zonal mean and subscripts without parentheses denote differentiation.

The EP flux is a conservative measure of the propagation of wave activity such that its divergence is zero under "nonacceleration conditions" (steady, conservative waves on a steady mean flow). Thus, an EP cross-section in which the EP flux is represented by arrows, and its divergence by contours, shows the net direction of wave propagation and the regions where nonacceleration conditions are invalid. From (1), it can be seen that the EP flux divergence is a measure of the wave-induced forcing of the mean state.

The graphical convention used for an EP cross section follows that used by Dunkerton *et al.* (1981). The EP flux divergence is weighted by the volume element dV, corresponding to a zonally symmetric portion of the atmosphere so that

$$\int \nabla \cdot \mathbf{F} dV = \int \Delta d\phi dz,$$

where

$$\Delta = \frac{\partial}{\partial \phi} \hat{F}_{(\phi)} + \frac{\partial}{\partial z} \hat{F}_{(z)}$$

$$= \frac{\partial}{\partial \phi} [2\pi a \cos\phi F_{(\phi)}] + \frac{\partial}{\partial z} [2\pi a^2 \cos\phi F_{(z)}]. \tag{6}$$

The quantity Δ is contoured in the (ϕ, z) plane, and arrows are drawn with horizontal and vertical components proportional to the terms in square brackets in (6). The pattern of arrows will appear nondivergent if and only if $\nabla \cdot \mathbf{F} = 0$.

The data used for this analysis were generated in an 18-level general circulation model of the Northern Hemisphere described by Hunt (1976). The model was set up for annual mean conditions prescribed by climatological zonal mean data for the radiation scheme. It included the hydrologic cycle but omitted all topographic features. The model was run for an extended period and the instantaneous values of model variables were stored every eight hours. These values were used to generate the zonal mean and flux quantities required, which were then time-averaged over nonoverlapping four day periods to reduce noise. In this paper, six sets of four-day means from days 288 to 312 of the model run are considered. These are part of the time series used in I and II, and cover the period of the largest variations in hemispheric mean eddy kinetic energy. The data are available on a grid with 15 equally spaced points from equator to pole and 18 unequally spaced sigma coordinate levels from the surface to ~40 km.

The time-mean climatology of this model has been described by Hunt (1976) and a good simulation of many of the zonal mean features of the atmosphere was obtained. Despite the use of annual mean radiation conditions, the model shows a bias toward winter conditions and the results are assumed to be representative of the winter half-year. The intensities of the tropospheric and stratospheric jets were well reproduced, but the jets were displaced slightly equatorward of their observed latitudes. The meridional circulation in the model agreed well with observations, both in intensity and structure, apart from some distortion of the Hadley cell by the equatorial boundary of the model. The energy balance revealed that the model lacked eddy energy compared to the atmosphere, probably due to the absence of topographic forcing in the model.

2. Results

The analysis of the time series of data from the general circulation model in I and II revealed a vacillation cycle in the model, particularly in the eddy kinetic energy. In II, it was shown that long and short term stratospheric variations were controlled by fluctuations of the vertical flux of wave energy from the troposphere. The wave energy flux is a function of the mean zonal flow (Eliassen and Palm, 1961) and, under nonacceleration conditions, the vertical flux of wave energy is not constant if the mean flow varies with height. Thus, the analysis of the vacillation cycle, using the wave energy flux, was not able to separate the effects of a changing mean flow from those due to a changing tropospheric wave source. Since the EP flux is conserved under nonacceleration conditions, it is a more useful diagnostic than the wave energy flux.

In II, there was some discussion on the correspondence between time variations of the vertical wave energy flux and the meridional wave heat flux, and

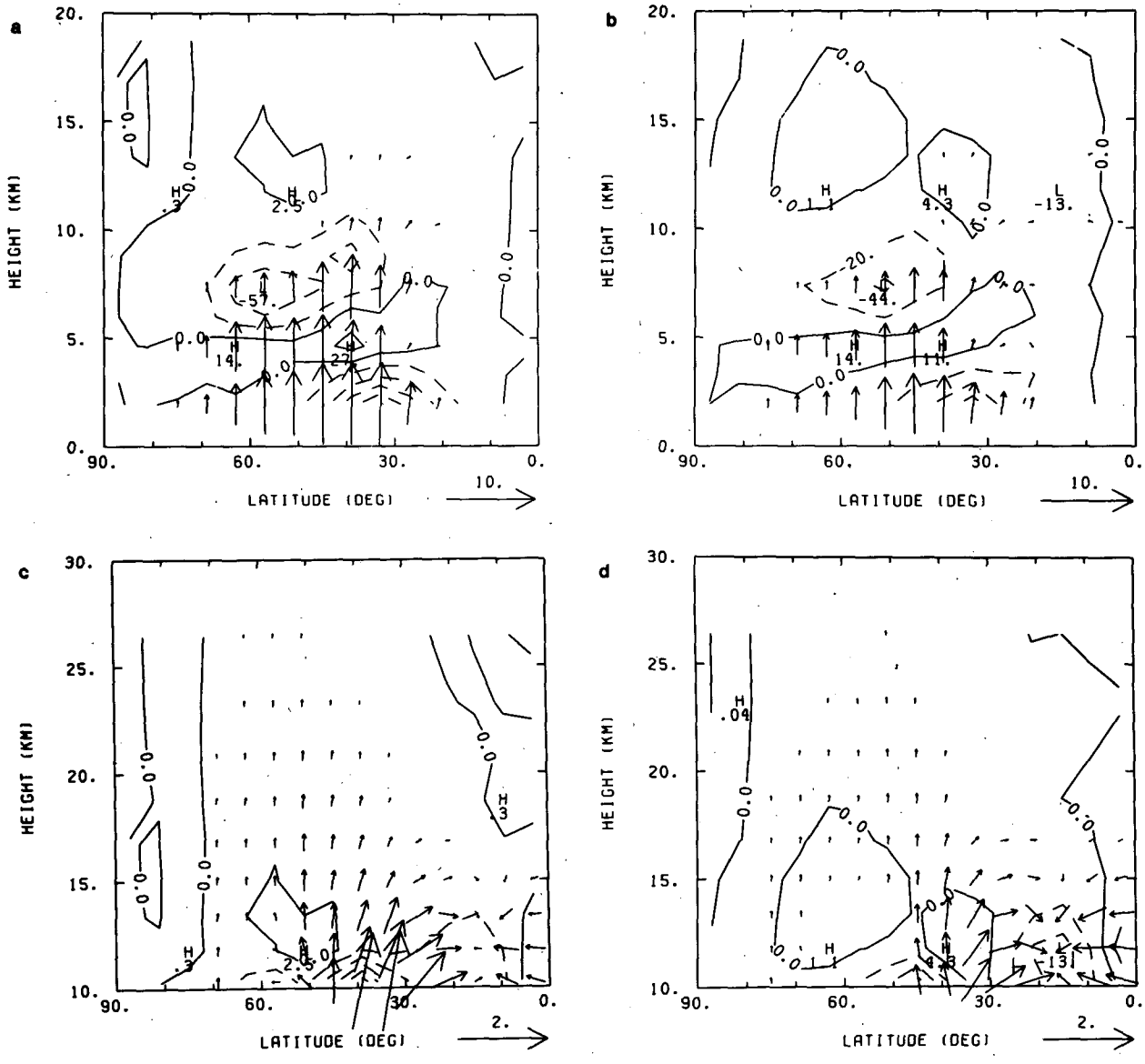

FIG. 2. Eliassen–Palm cross sections for the four-day periods centered at 302 days [(a) and (c)] and 310 days [(b) and (d)]. Contours represent the flux divergence quantity Δ defined by (6) in units of $10^{15}\ \rho_s\ m^4\ s^{-2}$. The contour interval is 20 units in (a) and (b) and 5 units in (c) and (d). The horizontal arrow scale for $\hat{F}_{(\phi)}$ in units of $10^{15}\ \rho_s\ m^4\ s^{-2}$ is indicated at the right below each diagram. A vertical arrow of the same length represents a flux $\hat{F}_{(z)}$, in $\rho_s\ m^5\ s^{-2}$, equal to that for the horizontal arrow multiplied by $4 \times 10^4\ \pi^{-1}$ m. The arrow scale in (c) and (d) is a factor of 5 larger than in (a) and (b). The vertical coordinate is the pressure–altitude z.

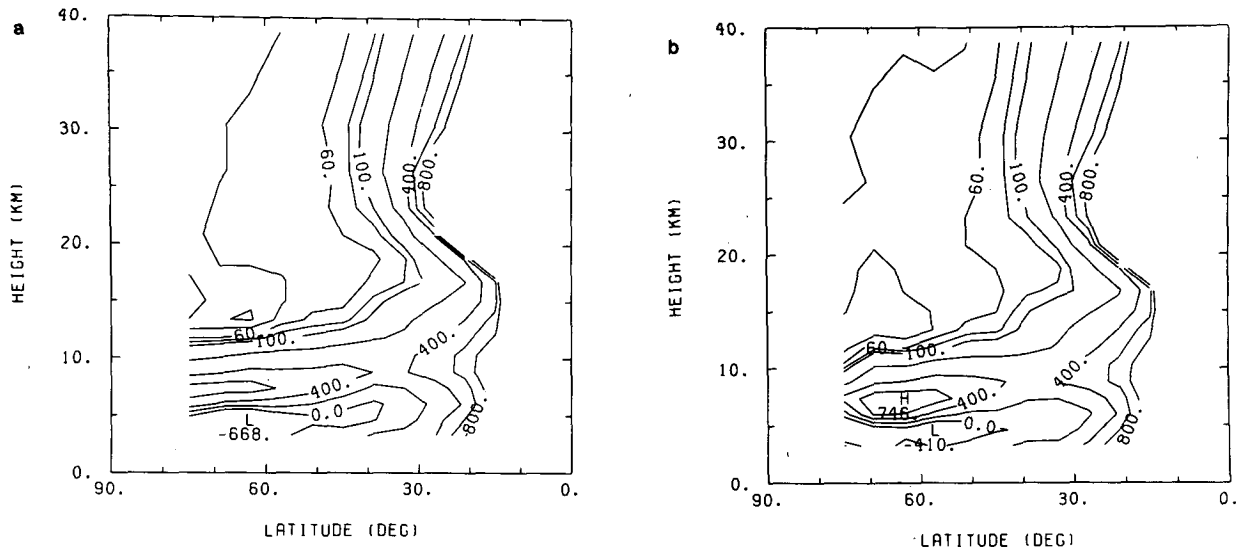

FIG. 3. Wave refractive index at (a) 302 and (b) 310 days. Contours represent the quantity $\tilde{Q}_0$ defined by (7) in nondimensional units. The contour interval is 20 between 0 and 100; and 200 between 200 and 800.

the lack of similar correspondence with variations of the meridional wave momentum flux. These relationships are apparent from the definitions of the EP flux in (5), and the link between the wave energy flux and the EP flux given by Eliassen and Palm (1961). In the simplest terms, the vertical flux of wave energy is proportional to the vertical EP flux, which is proportional to the meridional wave heat flux. It is the meridional component of the wave energy flux and not the vertical component which is proportional to the meridional wave momentum flux.

The time variations of four potential indicators of baroclinic wave activity in the troposphere during the vacillation cycle are shown in Fig. 1. The vertical shear of the zonal wind below the tropospheric jet and the meridional temperature gradient in the midlatitude lower troposphere in Figs. 1a and b are measures of the baroclinicity of the tropospheric mean state. They show a cycle in amplitude which leads that of the eddy kinetic energy by a short period less than four days. The vertical wave heat flux in Fig. 1c is a measure of baroclinic wave activity in the midlatitude lower troposphere and its time variation agrees well with that of the eddy kinetic energy described in II. The vertical EP flux in the midlatitude upper troposphere in Fig. 1d also shows the vacillation cycle, with amplitude varying by a factor of two during the cycle. These indicators and the eddy kinetic energy in II show large variations in tropospheric wave activity during the vacillation cycle.

EP cross sections for the four-day periods centered at 302 and 310 days, corresponding to a maximum and minimum in the vacillation cycle, are shown in Fig. 2. Figs. 2a and b show the cross sections in the height range from 0 to 20 km, while Figs. 2c and d show the height range from 10 to 30 km with increased arrow scale. The EP flux and flux divergence in the troposphere decrease by ~30% in amplitude during this period, but the flux direction changes little. The EP flux in the lower stratosphere decreases by ~50% during this period but, in the middle stratosphere, the amplitude variation is less. The EP flux directions are very similar at these two times. This suggests that the effect of the mean state on wave propagation does not change significantly during the vacillation cycle.

Another indicator of the effect of the mean state on wave propagation is the wave refractive index, defined, following Palmer (1982), by

$$\tilde{Q}_0 = (a\bar{q}_\phi/\bar{u} - f^2a^2/N^2H^2)(\sin^2\phi)^{-1}, \qquad (7)$$

where $\bar{q}_\phi$ is the meridional gradient of quasi-geostrophic potential vorticity and N is the Brunt-Väisälä frequency. Palmer has shown that $\tilde{Q}_0$ acts as a potential function so that integral curves of the EP flux are refracted up the gradient of $\tilde{Q}_0$. This definition is similar to the planetary wave refractive index used by Matsuno (1970). The refractive index at 302 and 310 days is shown in Fig. 3. There is very little difference in the upper troposphere and stratosphere between the two times. Thus, the effect of the mean state on wave propagation from the troposphere into the stratosphere is approximately constant during the vacillation cycle.

An analysis of the time variation of the terms in the transformed Eulerian-mean equations (1) and (2) has been made in order to understand the cause of the small mean state changes during the vacillation cycle. The analysis was performed at a number of

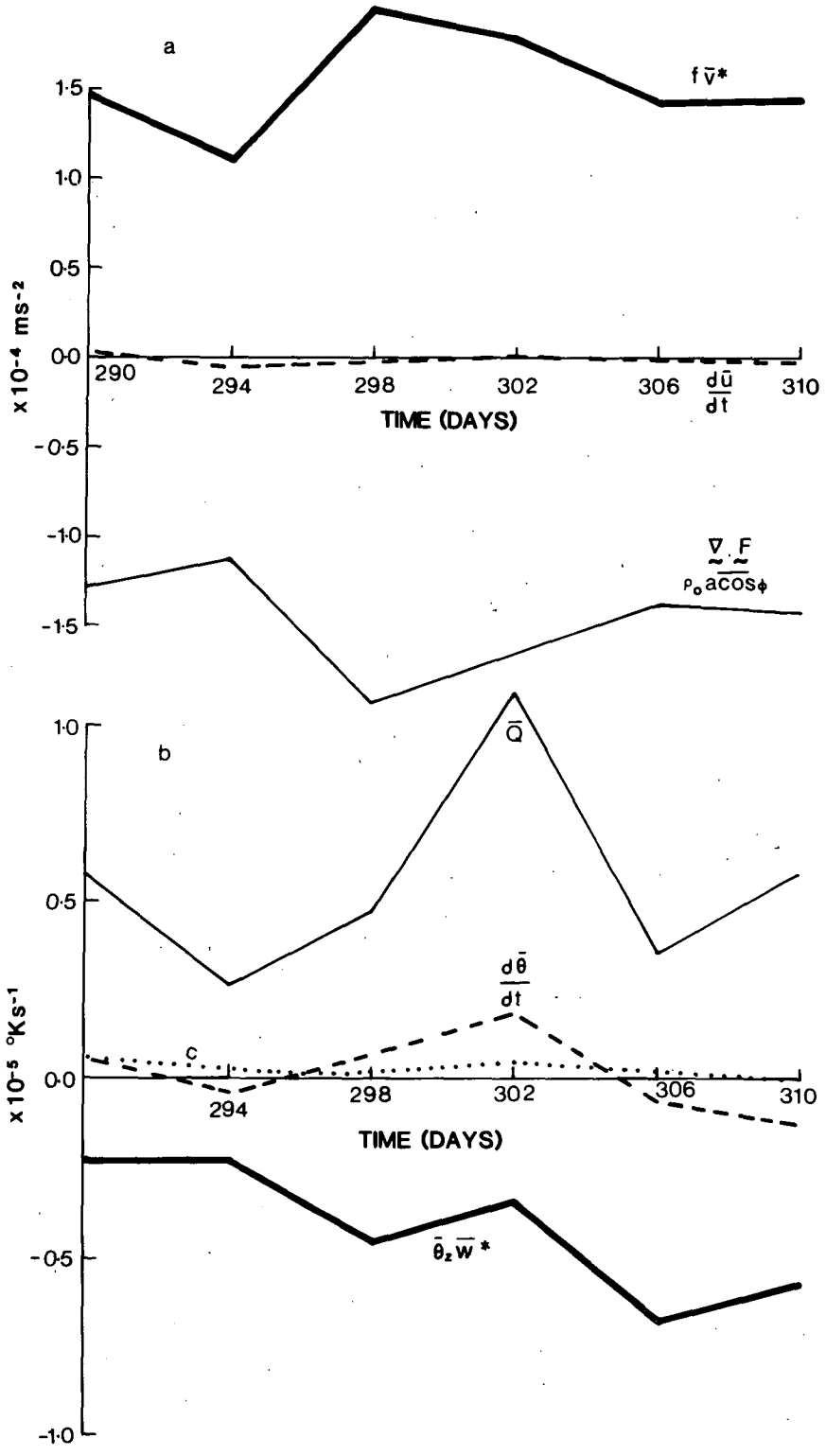

FIG. 4. (a) Time variation of the zonal flow budget for the zonal band from 45 to 51° and from 348 to 284 mb (z = 7.4 to 8.8). Terms are shown as in (1), apart from the dissipation $\bar{X}$. (b) Time variation of the temperature budget for the zonal band from 39 to 45° and from 626 to 516 mb (z = 3.3 to 4.6). Terms are shown as in (2), with c being the ageostrophic term corresponding to the convergence of vertical wave heat flux.

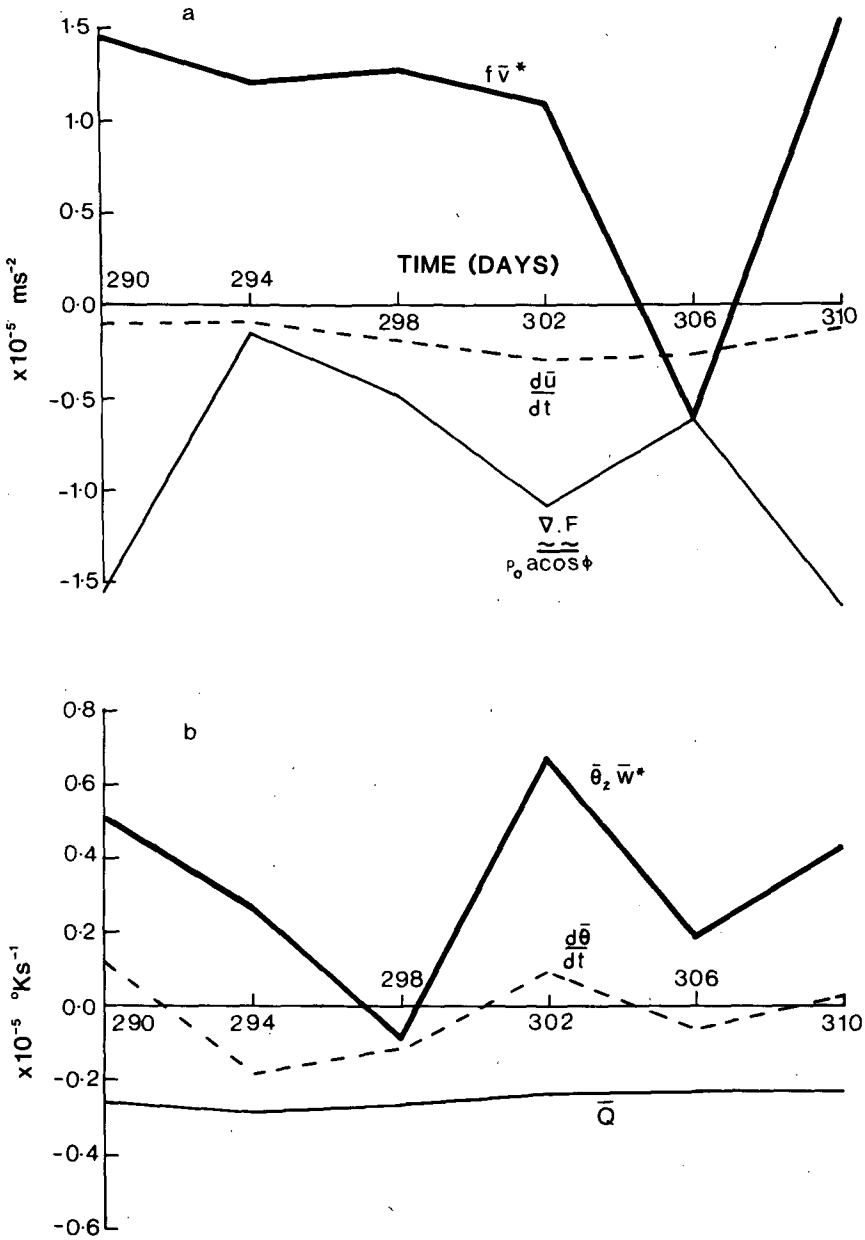

FIG. 5. Time variation of (a) zonal flow and (b) temperature budgets for the zonal band from 57 to 63° and from 36 to 23 mb (z = 23.3 to 26.4). Terms as in Fig. 4.

latitudes and heights in the model, and the results were all similar in the troposphere so budgets are presented here for two regions in the troposphere only. The zonal flow budget is analysed in the zonal band from 45 to 51° latitude and from 348 to 284 mb (z = 7.4 to 8.8), a region of large EP flux convergence and poleward residual circulation. The thermal budget is analysed in the zonal band from 39 to 45° latitude and from 626 to 516 mb (z = 3.3 to 4.6), a region of large diabatic heating and upward residual circulation.

For the zonal flow budget shown in Fig. 4a, the time variations of the wave-induced force on the mean flow and the Coriolis torque are large, but they remain in approximate balance. The zonal flow acceleration, calculated from the time change of the zonal flow, is more than an order of magnitude smaller than either of these terms. Also, its time variation is not correlated to that of the flux divergence term, which is different to that found in stratospheric model analyses by Dunkerton *et al.* (1981).

A similar balance occurs in the thermal budget,

shown in Fig. 4b. There are large time variations of the diabatic heating, mainly due to changes in the latent heat release, which are balanced by large and opposing changes in the residual vertical velocity. The calculated temperature change with time is correlated to, but much smaller than, the time variation of the diabatic heating.

Zonal flow and thermal budgets have also been carried out in a region in the high latitude stratosphere, for the zonal band from 57 to 63° latitude and from 36 to 23 mb (z = 23.3 to 26.4), at the maximum zonal wind at this level, and these are shown in Fig. 5. The terms in the zonal flow budget are much smaller than in the troposphere, and the balance between the wave-induced force on the mean flow and the Coriolis torque is not as good as in the troposphere. The zonal flow weakens throughout this period and its time variations are not related to those of the EP flux divergence. The model dissipation has not been included in this budget and it reduces the effect of variations of the flux divergence. For the thermal budget, there is a balance between the diabatic radiative cooling and adiabatic warming due to descent in the residual circulation. The radiative cooling is almost constant and the calculated time change of the temperature is correlated to the variations of the residual vertical velocity.

3. Summary

As shown by the wave refractive index and the direction of the EP flux, the effect of the mean state on wave propagation is approximately constant through the vacillation cycle. The intensity of baroclinic wave activity in the troposphere varies in response to changes in the baroclinicity of the tropospheric mean state. This leads to a vacillation of the effective tropospheric wave source and thus to changes in the amplitude of the wave activity propagating into the stratosphere. The vacillation cycle is apparently not due to wave, mean flow interaction in the stratosphere.

In the budget analysis of the vacillation cycle in the troposphere, there is a balance between the wave-induced force on the mean flow and the Coriolis torque, so that mean flow changes are small and cannot be inferred from the time variation of the EP flux divergence. A similar balance occurs in the thermal budget, so temperature changes are small but are related to time variations of the diabatic heating. Although this type of analysis has proved useful in the study of stratospheric warmings (Dunkerton *et al.*, 1981), it is not as useful in this case.

It is important to note that conclusions drawn from processes in this model may not apply to the atmosphere, since the model lacks topographic forcing, interhemispheric exchanges and seasonal variability.

Acknowledgments. I would like to thank B. G. Hunt for making available the data for this study, and Dr. R. A. Plumb for many helpful discussions.

REFERENCES

Andrews, D. G., and M. E. McIntyre, 1976: Planetary waves in horizontal and vertical shear: The generalized Eliassen–Palm relation and the mean zonal acceleration. *J. Atmos. Sci.*, **33,** 2031–2048.

Dunkerton, T., C.-P. F. Hsu and M. E. McIntyre, 1981: Some Eulerian and Lagrangian diagnostics for a model stratospheric warming. *J. Atmos. Sci.*, **38,** 819–843.

Edmon, H. J., B. J. Hoskins and M. E. McIntyre, 1980: Eliassen–Palm cross sections for the troposphere. *J. Atmos. Sci.*, **37,** 2600–2616.

Eliassen, A., and E. Palm, 1961: On the transfer of energy in stationary mountain waves. *Geofys. Publ.*, **22,** 1–23.

Hunt, B. G., 1976: Experiments with a stratospheric general circulation model: Part IV. Inclusion of the hydrologic cycle. *Mon. Wea. Rev.*, **104,** 333–350.

——, 1978a: Atmospheric vacillations in a general circulation model. I: The large-scale energy cycle. *J. Atmos. Sci.*, **35,** 1133–1143.

——, 1978b: Atmospheric vacillations in a general circulation model. II: Tropospheric–stratospheric coupling and stratospheric variability. *J. Atmos. Sci.*, **35,** 2052–2067.

Matsuno, T., 1970: Vertical propagation of stationary planetary waves in the winter Northern Hemisphere. *J. Atmos. Sci.*, **27,** 871–883.

Palmer, T. N., 1982: Properties of the Eliassen-Palm flux for planetary scale motions. *J. Atmos. Sci.*, **39,** 992–997.